NERC
NORTH AMERICAN ELECTRIC RELIABILITY CORPORATION

Supplemental Geomagnetic Disturbance Event Description

Project 2013-03 GMD Mitigation

June 2017

RELIABILITY | ACCOUNTABILITY


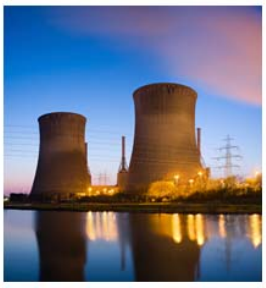

3353 Peachtree Road NE
Suite 600, North Tower
Atlanta, GA 30326
404-446-2560 | www.nerc.com

Table of Contents

Preface

The North American Electric Reliability Corporation (NERC) is a not-for-profit international regulatory authority whose mission is to assure the reliability and security of the bulk power system (BPS) in North America. NERC develops and enforces Reliability Standards; annually assesses seasonal and long-term reliability; monitors the BPS through system awareness; and educates, trains, and certifies industry personnel. NERC's area of responsibility spans the continental United States, Canada, and the northern portion of Baja California, Mexico. NERC is the Electric Reliability Organization (ERO) for North America, subject to oversight by the Federal Energy Regulatory Commission (FERC) and governmental authorities in Canada. NERC's jurisdiction includes users, owners, and operators of the BPS, which serves more than 334 million people.

The North American BPS is divided into eight Regional Entity (RE) boundaries as shown in the map and corresponding table below.

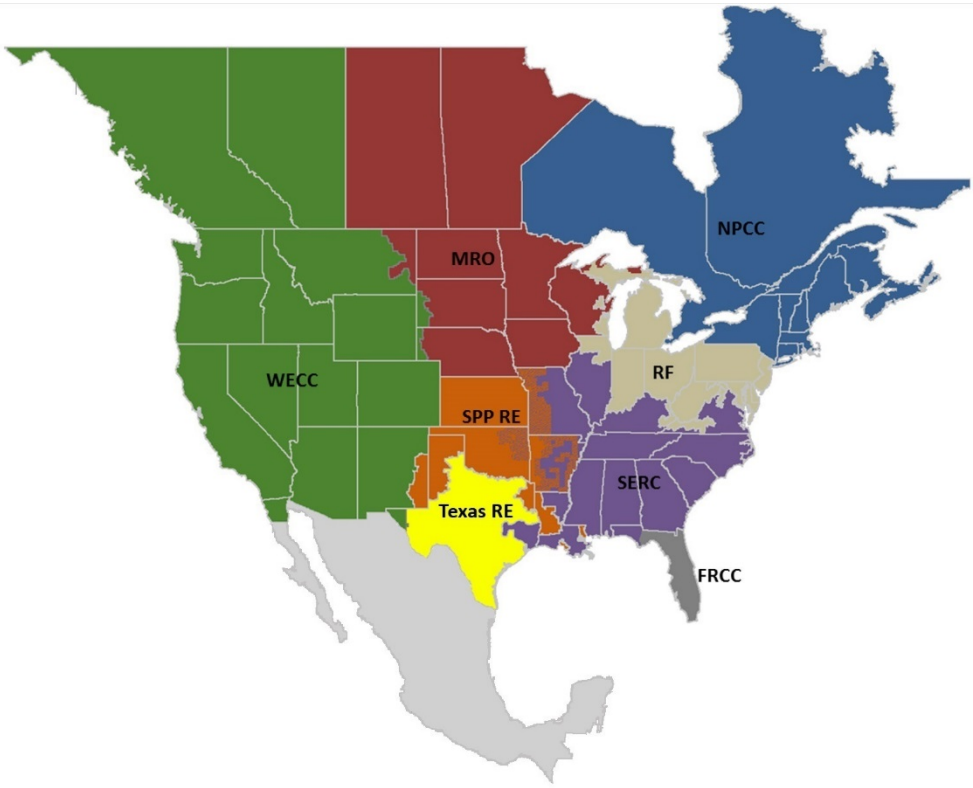

The North American BPS is divided into eight RE boundaries. The highlighted areas denote overlap as some load-serving entities participate in one Region while associated transmission owners/operators participate in another.

FRCC	Florida Reliability Coordinating Council
MRO	Midwest Reliability Organization
NPCC	Northeast Power Coordinating Council
RF	ReliabilityFirst
SERC	SERC Reliability Corporation
SPP RE	Southwest Power Pool Regional Entity
Texas RE	Texas Reliability Entity
WECC	Western Electricity Coordinating Council

Introduction

Background

Proposed TPL-007-2 includes requirements for entities to perform two types of GMD Vulnerability Assessments to evaluate the potential impacts of GMD events on the Bulk Electric System (BES):

- The benchmark GMD Vulnerability Assessment is based on the benchmark GMD event associated with TPL-007-1 which was approved by the Federal Energy Regulatory Commission (FERC) in Order No. 830 in September 2016. The benchmark GMD event is derived from spatially-averaged geoelectric field values to address potential wide-area effects that could be caused by a severe 1-in-100 year GMD event.[1]
- The supplemental GMD Vulnerability Assessment, based on the supplemental GMD event described in this white paper, is used by entities to evaluate localized enhancements of geomagnetic field during a severe GMD event that "could potentially affect the reliable operation of the Bulk-Power System".[2] Localized enhancements of geomagnetic field can result in geoelectric field values above the spatially-averaged benchmark in a local area.

The purpose of the supplemental geomagnetic disturbance (GMD) event description is to provide a defined event for assessing system performance for a GMD event which includes a local enhancement of the geomagnetic field. In addition to varying with time, geomagnetic fields can be spatially non-uniform with higher and lower strengths across a region. This spatial non-uniformity has been observed in a number of GMD events, so localized enhancement of field strength above the average value is considered. The supplemental GMD event defines the geomagnetic and geoelectric field values used to compute geomagnetically-induced current (GIC) flows for a supplemental GMD Vulnerability Assessment.

General Characteristics

The supplemental GMD event described herein takes into consideration observed characteristics of a local geomagnetic field enhancement, recognizing that the science and understanding of these events is evolving. Based on observations and initial assessments, the characteristics of local enhancements include:

- Geographic area – The extent of local enhancements is on the order of 100km in North-South (latitude) direction but longer in East-West (longitude) direction. Further description of the geographic area is provided later in the white paper.
- Amplitude – The amplitude of the resulting geoelectric field is significantly higher than the geoelectric field that is calculated in the spatially-averaged Benchmark GMD event.
- Duration – The local enhancement in the geomagnetic field occurs over a time period of 2-5 minutes.
- Geoelectric field waveform – The supplemental GMD event waveform is the benchmark GMD event waveform with the addition of a local enhancement. The added local enhancement has amplitude and duration characteristics described above. The geoelectric field waveform has a strong influence on the hot spot heating of transformer windings and structural parts since thermal time constants of the transformer and time to peak of storm maxima are both on the order of minutes. The frequency content of the rate of change of the magnetic field (dB/dt) is a function of the waveform, which in turn has a direct effect on the geoelectric field since the earth response to dB/dt is frequency-dependent. As with the benchmark GMD event, the supplemental GMD event waveform is based on magnetic field data recorded by the Natural Resources Canada (NRCan) Ottawa (OTT) geomagnetic observatory during the March 13-

[1] See *Benchmark Geomagnetic Disturbance Event Description* white paper, May 12, 2016. Filed by NERC in RM 15-11 on June 28, 2016.

[2] See Order No. 830 P. 47. On September 22, 2016, FERC directed NERC to develop modifications to the benchmark GMD event, included in TPL-007-1, such that assessments would not be based solely on spatially averaged data.

14 1989 event. This GMD event data was selected because analysis of recorded events indicates that the OTT observatory data for this period provides conservative results when performing thermal assessments of power transformers.[3]

[3] See *Benchmark Geomagnetic Disturbance Event Description* white paper, page 5 and Appendix I.

Supplemental GMD Event Description

Severe geomagnetic disturbance events are high-impact, low-frequency (HILF) events [1]; thus, GMD events used in system planning should consider the probability that the event will occur, as well as the impact or consequences of such an event. The supplemental GMD event is composed of the following elements: 1) a reference peak geoelectric field amplitude (V/km) derived from statistical analysis of historical magnetometer data; 2) scaling factors to account for local geomagnetic latitude; 3) scaling factors to account for local earth conductivity; and 4) a reference geomagnetic field time series or waveform to facilitate time-domain analysis of GMD impact on equipment.

Supplemental GMD Event Geoelectric Field Amplitude

The supplemental GMD event field amplitude was determined through statistical analysis using the plane wave method [2]-[9] of geomagnetic field measurements from geomagnetic observatories in northern Europe [10] and the reference (Quebec) earth model shown in **Table 1** [11], supplemented by data from Greenland, Denmark and Alaska. For details of the statistical considerations, see Appendix I. The Quebec earth model is generally resistive and the geological structure is relatively well understood.

Table 1: Reference Earth Model (Quebec)

Thickness (km)	Resistivity (Ω-m)
15	20,000
10	200
125	1,000
200	100
∞	3

The statistical analysis (see Appendix I) resulted in conservative peak geoelectric field amplitude of approximately 12 V/km. For steady-state GIC and load flow analysis, the direction of the geoelectric field is assumed to be variable meaning that it can be in any direction (Eastward, Northward, or a vectorial combination thereof).

The regional geoelectric field peak amplitude, E_{peak}, to be used in calculating GIC in the GIC system model can be obtained from the reference value of 12 V/km using the following relationship

$$E_{peak} = 12 \times \alpha \times \beta_s \text{ (V/km)} \quad (1)$$

where α is the scaling factor to account for local geomagnetic latitude, and β_S is a scaling factor for the supplemental GMD event to account for the local earth conductivity structure (see Appendix II).

Supplemental Geomagnetic Field Waveform

The supplemental geomagnetic field waveform is the benchmark geomagnetic field waveform with the addition of a local enhancement. Both the benchmark and supplemental geomagnetic field waveforms are used to calculate the GIC time series, GIC(t), required for transformer thermal impact assessments. The supplemental waveform includes a local enhancement, inserted at UT 1:18 March 14 in **Figure 1** below. This time corresponds to the largest calculated geoelectric fields during the benchmark GMD event. The amplitude of the local enhancement is based on a statistical analysis of a number of GMD events, discussed in Appendix I**.** The duration of the enhancement is based on the characteristics of observed localized enhancements as discussed in Appendix I.

The geomagnetic latitude of the Ottawa geomagnetic observatory is 55°; therefore, the amplitude of the geomagnetic field measurement data with a local enhancement was scaled up to the 60° reference geomagnetic latitude (see **Figure 1**) such that the resulting peak geoelectric field amplitude computed using the reference earth model was 12 V/km (see **Figure 2**). Sampling rate for the geomagnetic field waveform is 10 seconds.

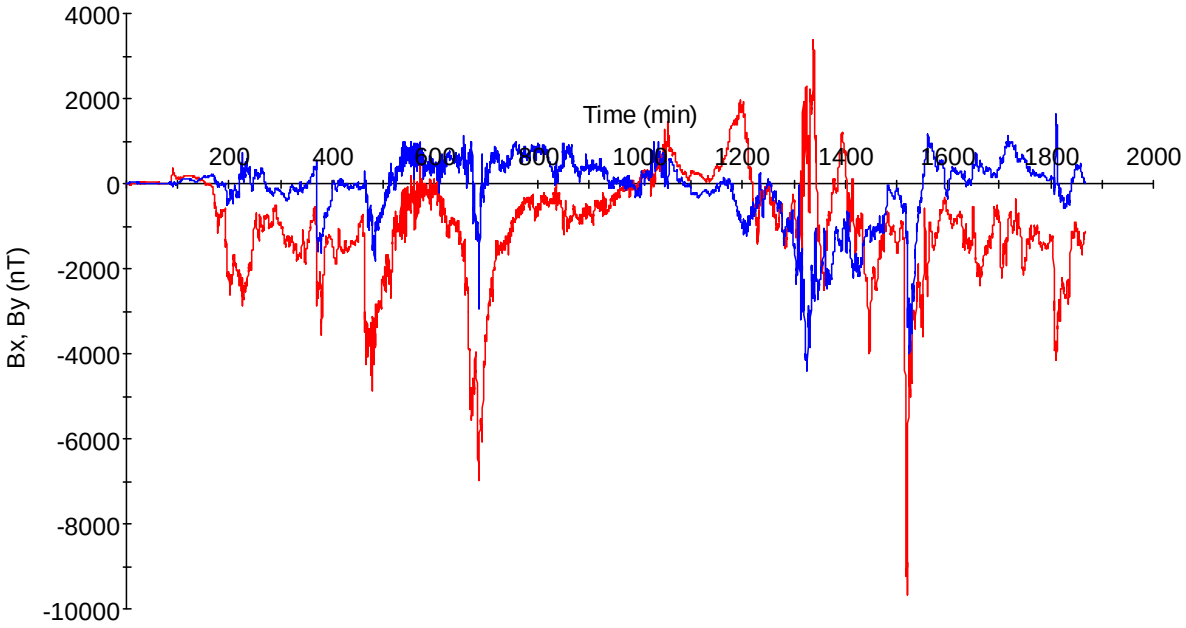

Figure 1: Supplemental Geomagnetic Field Waveform
Red B_x (Northward), Blue B_y (Eastward),
Referenced to pre-event quiet conditions

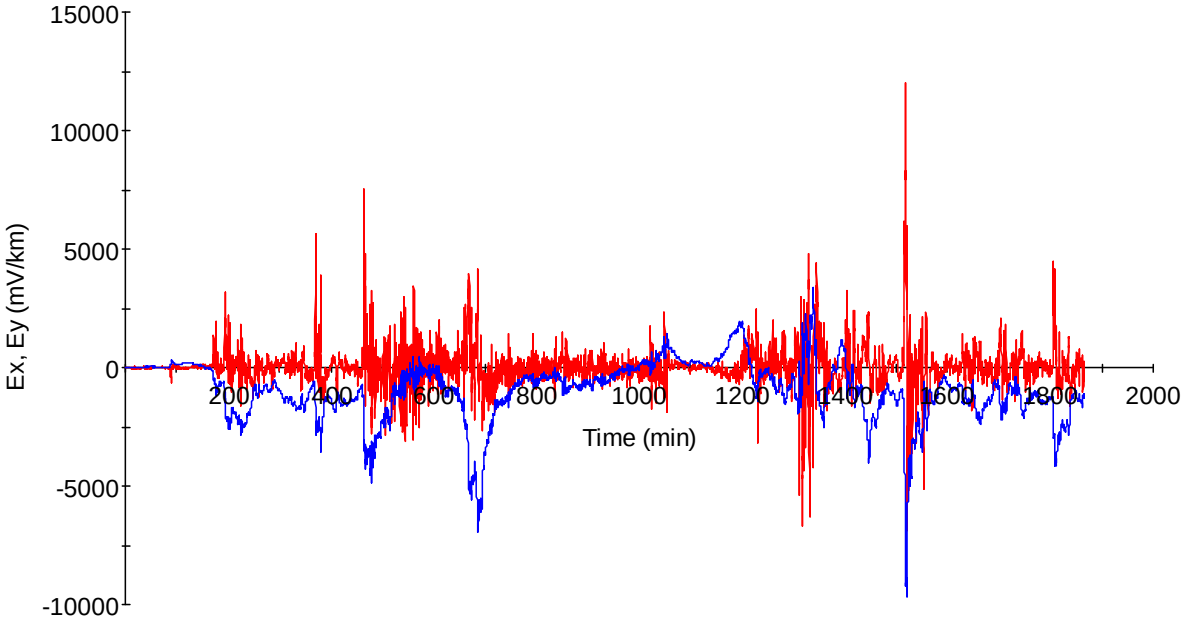

Figure 2: Supplemental Geoelectric Field Waveform
Red E_y (Eastward), Blue E_x (Northward)

Appendix I – Technical Considerations

The following sections describe the technical justification of the assumptions that were made in the development of the supplemental GMD event.

Statistical Considerations

The peak geoelectric field amplitude of the supplemental GMD event was determined through statistical analysis of modern 10-second geomagnetic field data and corresponding calculated geoelectric field amplitudes. The objective of the analysis was to estimate the geoelectric field amplitude that is associated with a 1 in 100 year frequency of occurrence. The same data set and similar statistical techniques were used in determining the peak geoelectric field amplitude of the benchmark GMD event, including extreme value analysis discussed in the following section.[4] The fundamental difference in the supplemental GMD event amplitude is that it is based on observations taken at each individual station (i.e., localized measurements), in contrast with the spatially averaged geoelectric fields used in the *Benchmark Geomagnetic Disturbance Event Description* white paper.[5]

[4] See *Benchmark Geomagnetic Disturbance Event Description* white paper, Appendix I, pages 8-13.

[5] Averaging the geoelectric field values of stations in geographic groups is referred to as spatial averaging in the *Benchmark Geomagnetic Disturbance Event Description.* Spatial averaging was used to characterize GMD events over a geographic area relevant to the interconnected transmission system for purposes of assessing area effects such as voltage collapse and widespread equipment risk. See *Benchmark Geomagnetic Disturbance Event Description* white paper, Appendix I, pages 9-10.

Extreme Value Analysis

The objective of extreme value analysis is to describe the behavior of a stochastic process at extreme deviations from the median. In general, the intent is to quantify the probability of an event more extreme than any previously observed. In particular, we are concerned with estimating the 95% confidence interval of the maximum geoelectric field amplitude to be expected within a 100-year return period.[6]

The data set consists of 23 years of daily maximum geoelectric field amplitudes derived from individual stations in the IMAGE magnetometer chain, using the Quebec earth model as a reference. **Figure I-1** shows a scatter plot of geoelectric field amplitudes that exceed 2 V/km across the IMAGE stations. The plot indicates that there is seasonality in extreme observations associated with the 11-year solar cycle.

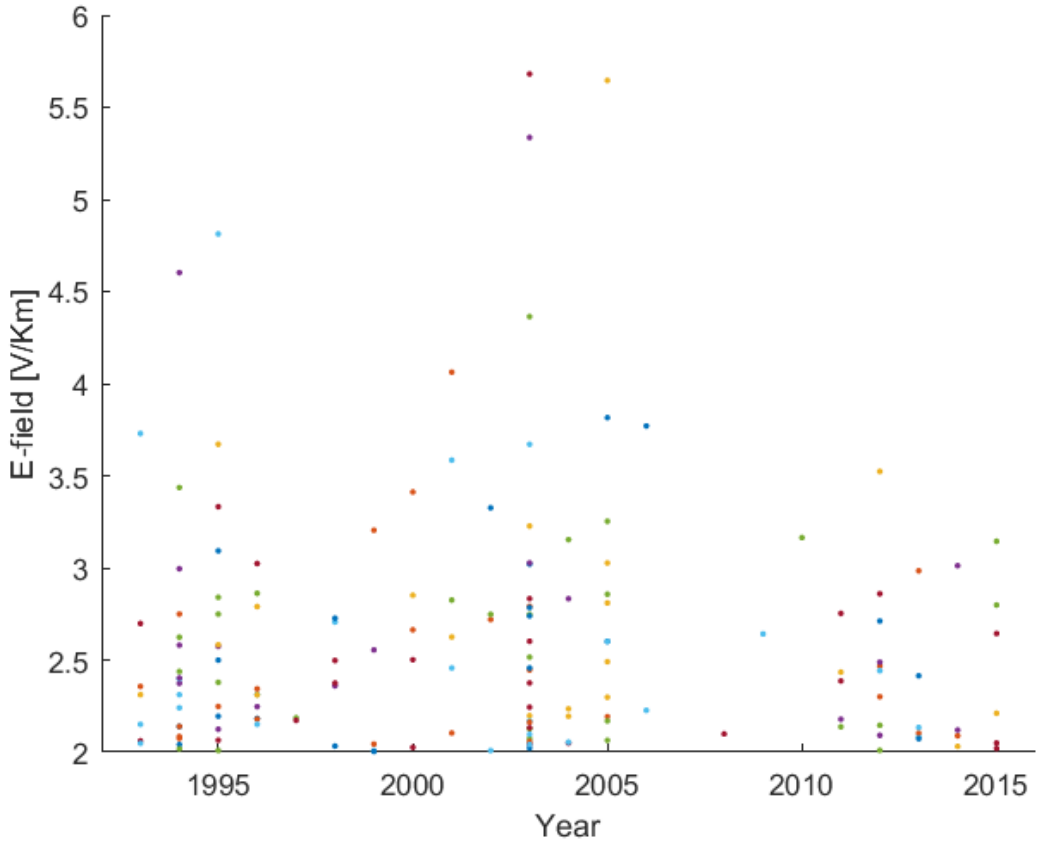

Figure I-1: Scatter Plot of Geoelectric Fields that Exceed a 2 V/km Threshold
Data source: IMAGE magnetometer chain from 1993-2015.

[6] A 95 percent confidence interval means that, if repeated samples were obtained, the return level would lie within the confidence interval for 95 percent of the samples.

Several statistical methods can be used to conduct extreme value analysis. The most commonly applied include: Generalized Extreme Value (GEV), Point Over Threshold (POT), R-Largest, and Point Process (PP). In general, all methods assume independent and identically distributed (iid) data [12].

Table I-1 shows a summary of the estimated parameters and return levels obtained from different statistical methods. The parameters were estimated using the Maximum Likelihood Estimator (MLE). Since the distribution parameters do not have an intuitive interpretation, the expected geoelectric field amplitude for a 100-year return period is also included in **Table I-1**. The 95% confidence interval of the 100-year return level was calculated using the delta method and the profile likelihood. The delta method relies on the Gaussian approximation to the distribution of the MLE; this approximation can be poor for long return periods. In general, the profile likelihood provides a better description of the return level.

Table I-1: Extreme Value Analysis

Statistical Model	Estimated Parameters	Hypothesis Testing	100 Year Return Level Mean [V/km]	95% CI Delta [V/km]	95% CI P-Likelihood [V/km]
(1) GEV	μ=2.976 (0.193) σ=0.829 (0.1357) ξ=-0.0655 (0.1446)	H0: ξ=0 *p* = 0.66	6.9	[4.3, 8.2]	[5.2, 11.4]
(2) GEV, reparametrization $\mu = \beta_0 + \beta_1 \cdot \sin\left(\frac{t}{T} + \phi\right)$	β_0= 2.964 (0.151) β_1=0.582 (0.155) σ=0.627 (0.114) ξ=0.09 (0.183)	H0: β_1=0 *p* = 0.00 H0: ξ=0 *p* = 0.6	7.1	[4, 10.2]	[5.5, 18]
(3) POT, threshold=2 V/km 3 day decluster. 143 observations > 2V/km.	σ=0.592 (0.074) ξ=0.077 (0.093)		6.9	[4.5, 9.4]	[5.4, 11.9]
(4) POT, threshold=2V/km reparametrization, $\sigma = \beta_0 + \beta_1 \cdot \sin\left(\frac{t}{T} + \phi\right)$	β_0=0.58 (0.073) β_1=0.107 (0.082) ξ=0.037 (0.097)	H0: B1=0 *p* = 0.2	7	[4.6, 9.3]	[5.5, 11.7]

Statistical model (1) in **Table I-1** is the traditional GEV estimation using blocks of 1 year maxima; i.e., only 23 data points are used in the estimation. The mean expected amplitude of the geoelectric field for a 100-year return level is approximately 7 V/km. Since GEV works with blocks of maxima, it is typically regarded as a wasteful approach.

As discussed previously, GEV assumes that the data is iid. Based on the scatter plot shown in **Figure I-1**, the iid statistical assumption is not warranted by the data. Statistical model (2) in **Table I-1** is a reparametrization of the GEV distribution contemplating the 11-year seasonality in the mean,

$$\mu = \beta_0 + \beta_1 \cdot \sin\left(\frac{t}{T} + \phi\right)$$

where β_0 represents the offset in the mean, β_1 describes the 11-year seasonality, *T* is the period (11 years), and ϕ is a constant phase shift.

A likelihood ratio test is used to test the hypothesis that β_1 is zero. The null hypothesis, H0: $\beta_1=0$, is rejected with a p-value of 0.0032; as expected, the 11-year seasonality has explanatory power. The blocks of maxima during the solar minimum are better represented in the reparametrized GEV. The mean return level is still 7 V/km, but the confidence interval is wider, [5.5, 18] V/km for the profile likelihood (calculated at solar maximum).

Statistical model (3) in **Table I-1** is the traditional POT estimation using a threshold *u* of 2 V/km; the data was declustered using a 1-day run. The data set consists of normalized excesses over a threshold, and therefore, the sample size for POT is increased if more than one extreme observation per year is available (in the GEV approach, only the maximum observation over the year was taken; in the POT method, a single year can have multiple observations over the threshold). The selection of the threshold *u* is a compromise between bias and variance. The asymptotic basis of the model relies on a high threshold; too low a threshold will likely lead to bias. On the other hand, too high a threshold will reduce the sample size and result in high variance. A threshold of 2V/km was determined to be a good choice, giving rise to 143 observations above the threshold.

The mean return level for statistical model (3), ~7 V/km, is consistent with the GEV estimates. However, due to the larger sample size the POT method is more efficient rendering a confidence interval of [5.4, 11.9] V/km for the profile likelihood method.

In an attempt to cope with potential heteroskedasticity in the data, a reparametrization of POT is proposed in statistical model (4) in **Table I-1**,

$$\sigma = \alpha_0 + \alpha_1 \cdot \sin\left(\frac{t}{T} + \phi\right)$$

where α_0 represents the offset in the standard deviation, α_1 describes the 11-year seasonality, *T* is the period ($365.25 \cdot 11$), and ϕ is a constant phase shift.

The parameter α_1 is not statistically significant; the null hypothesis, H0: $\alpha_1=0$, is not rejected with a p-value of 0.2. The proposed reparametrization does not have explanatory power, and consequently, the mean return level 7 V/km and confidence intervals remain virtually unchanged [5.5, 11.7]. As a final remark, it is emphasized that the confidence interval obtained using the profile likelihood is preferred over the delta method.

Figure I-2 shows the profile likelihood of the 100-year return level of statistical model (3). Note that the profile likelihood is highly asymmetric with a positive skew, rendering a larger upper limit for the confidence interval. Recall that the delta method assumes a normal distribution for the MLEs, and therefore, the confidence interval is symmetric around the mean.

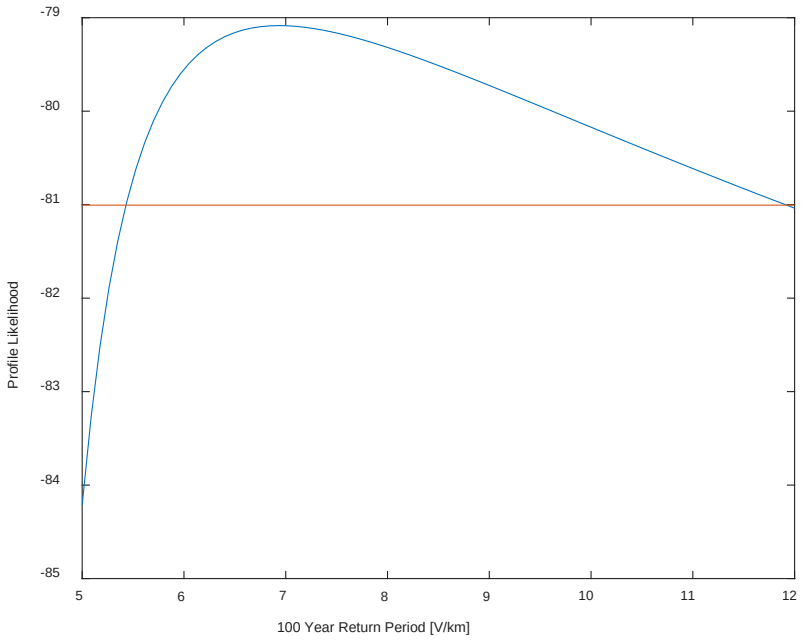

Figure I-2: Profile Likelihood for 100-year Return Level for Statistical Model (3)

To conclude, the traditional GEV (1) is misspecified; the statistical assumptions (iid) are not warranted by the data. The model was reparametrized to cope with seasonality in the data. Statistical models (3) and (4) better utilize the available extreme measurements and they are therefore preferred over statistical model (2). A geoelectric field amplitude of 12 V/km is selected for the supplemental GMD event to represent the upper limit of the 95 percent confidence interval for a 100-year return interval.

Spatial Considerations

The spatial structure of high-latitude geomagnetic fields can be very complex during strong geomagnetic storm events [13]-[14]. One reflection of this spatial complexity is localized geomagnetic field enhancements (local enhancements) that result in high amplitude geoelectric fields in regions of a few hundred kilometers. **Figure I-3** illustrates this spatial complexity of the storm-time geoelectric fields.[7] In areas indicated by the bright red location, the geoelectric field can be substantially larger than at neighboring locations. These enhancements are primarily the result of external (geomagnetic field) conditions, and not local geological factors such as coastal effects.[8]

[7] **Figure I-3** is for illustration purposes only, and is not meant to suggest that a particular area is more likely to experience a localized enhanced geoelectric field. The depiction is not to scale.

[8] Localized externally-driven geomagnetic phenomena should not be confused with localized geoelectric field enhancements due to complex electromagnetic response of the ground to external excitation. Complex 3D geological conditions such as those at coastal regions can lead to localized geoelectric field enhancements but those are not considered here.

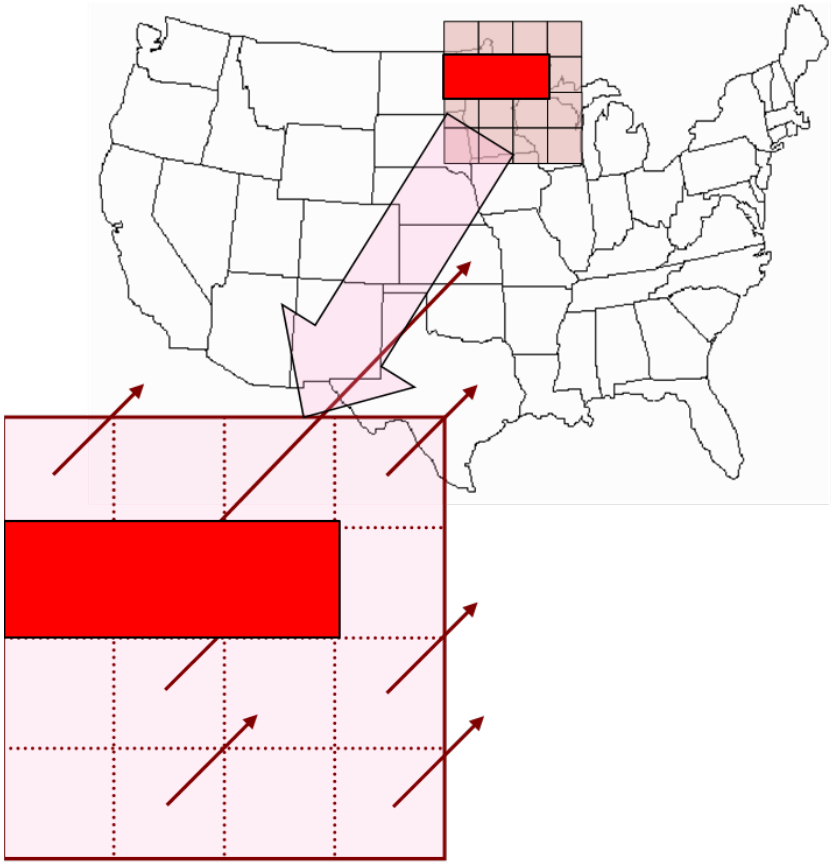

Figure I-3: Illustration of the Spatial Scale between Localized Enhancements and Larger Spatial Scale Amplitudes of Geoelectric Field during a Strong Geomagnetic Storm.
In this figure, the red rectangle illustrates a spatially localized field enhancement.

The supplemental GMD event is designed to address local effects caused by a severe GMD event, such as increased var absorption and voltage depressions.

A number of GMD events were analyzed to identify the basic characteristics of local enhancements. Three (3) solar storms studied and described below are:

- March 13, 1989
- October 29-30, 2003
- March 17, 2015

Four localized events within those storms were identified and analyzed. Geomagnetic field recordings were collected for these storms and the geoelectric field was computed using the 1D plane wave method and the reference Quebec ground model. In each case, a local enhancement was correlated, generally oriented parallel to the westward ionospheric electrojet associated with ongoing larger scale geomagnetic activity. (See **Figures I-4 – I-7** below)

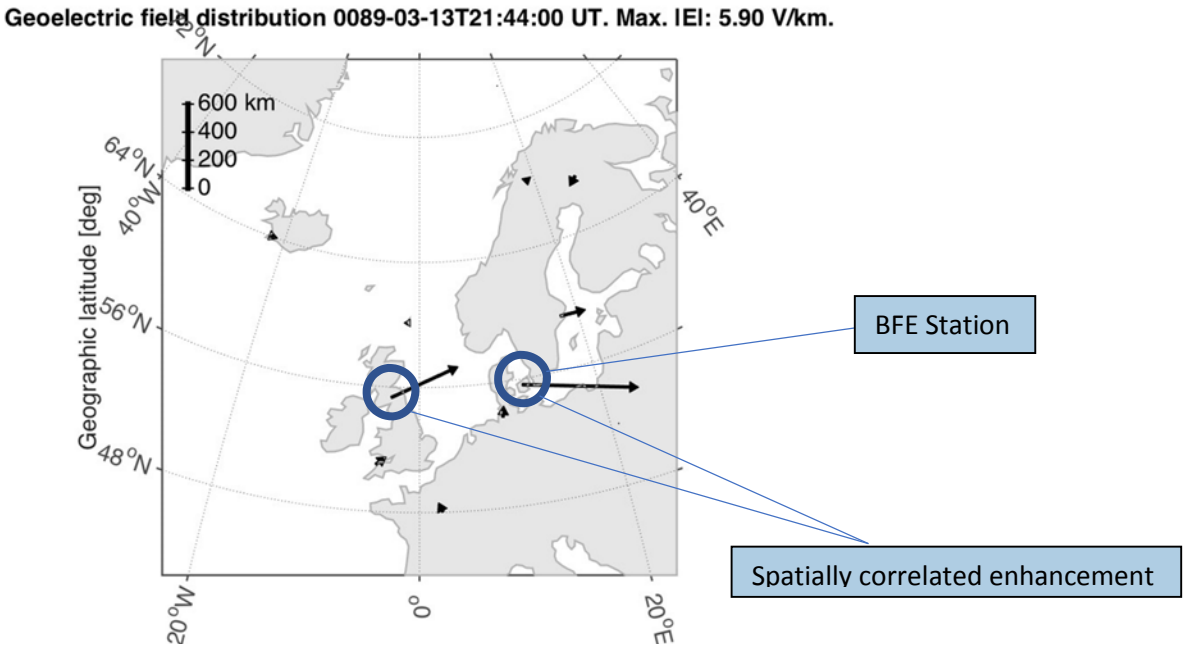

Figure I-4: March 13, 1989, at 21:44 UT, Brorfelde (BFE), Denmark

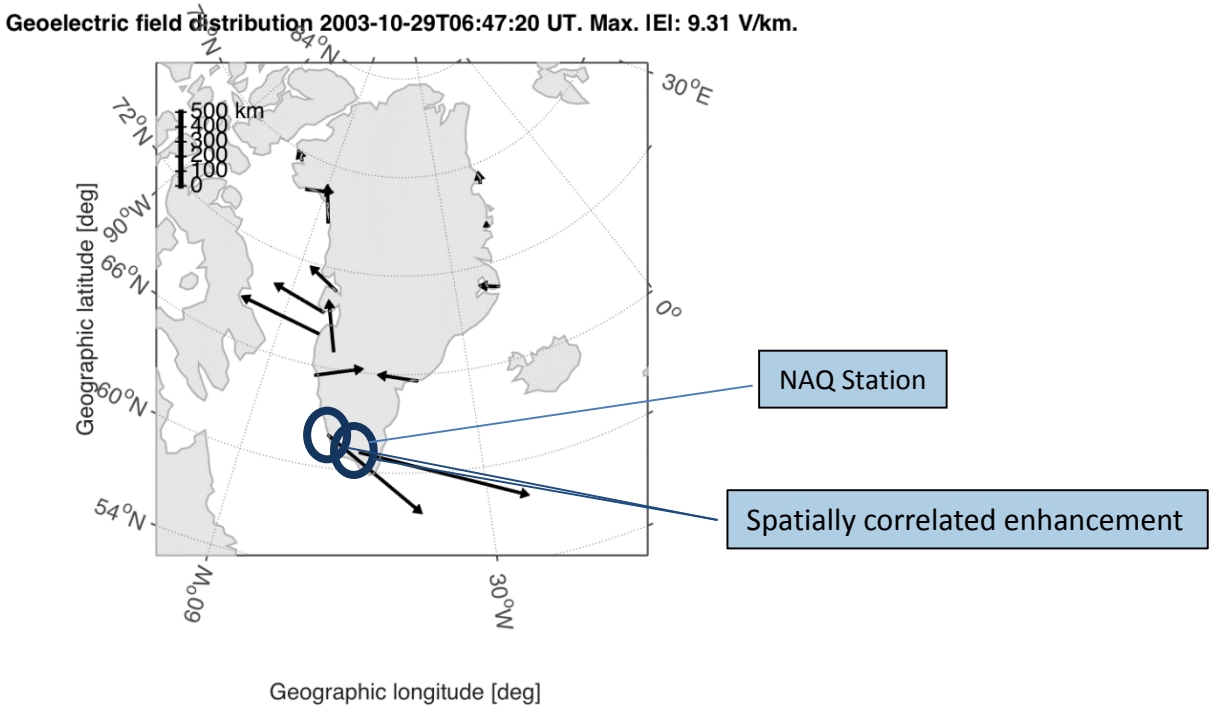

Figure I-5: October 29, 2003, at 06:47 UT, Narsarsuaq (NAQ), Greenland

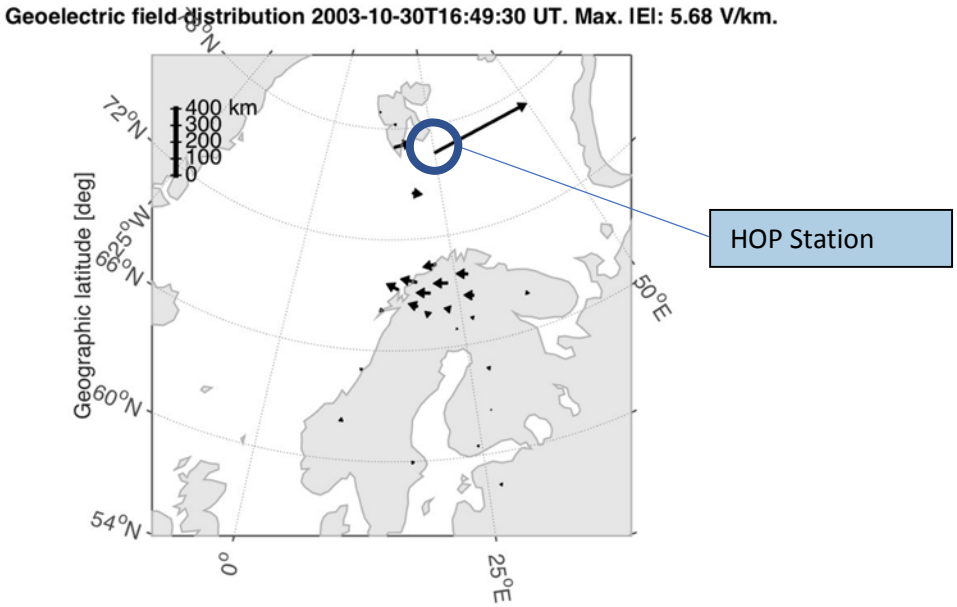

Figure I-6: October 30, 2003, at 16:49UT, Hopen Island (HOP), Svalbard, Norway

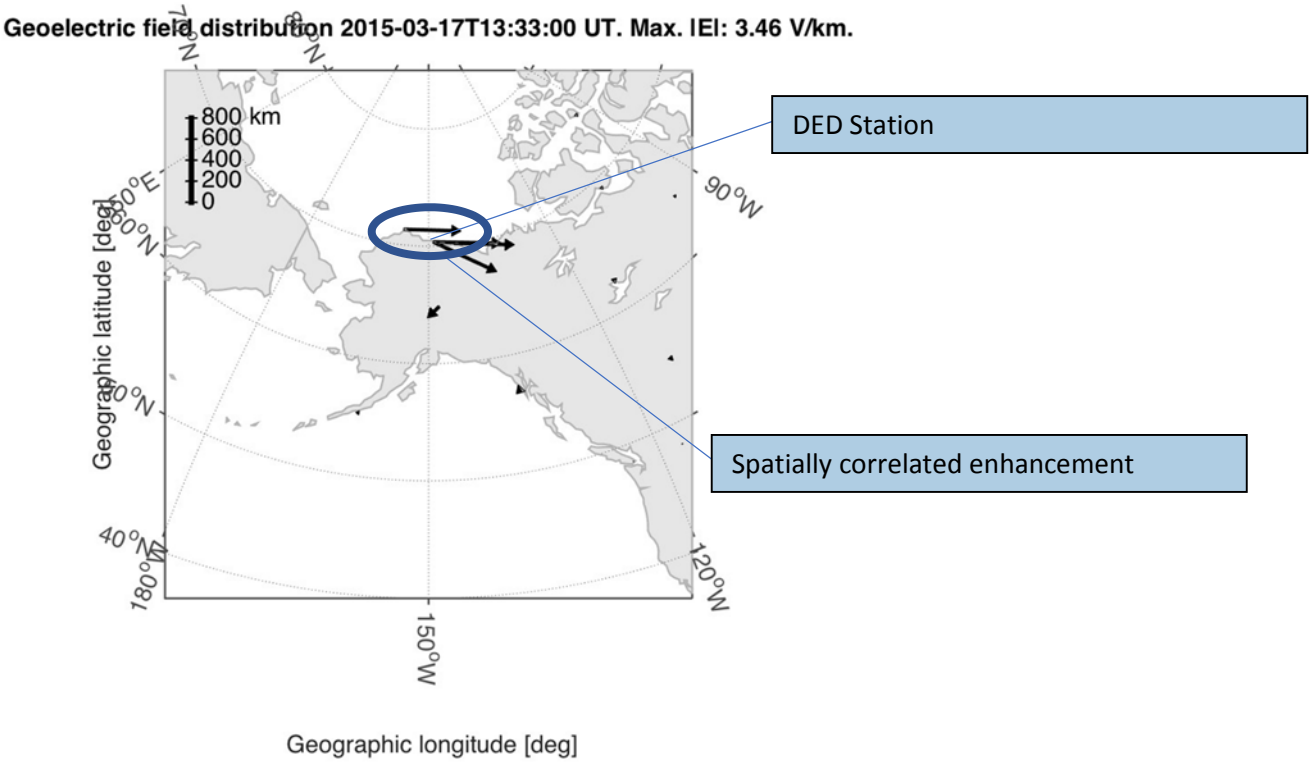

Figure I-7: March 17, 2015, at 13:33 UT, Deadhorse, Alaska

All of the above events were analyzed by reviewing the time series magnetic field data and transforming it to an electric field and focusing on the time period of the spatially correlated local enhancement. There were apparent similarities in the character of the local enhancements. The local enhancements occurred during peak periods of

geomagnetic activity and were distinguished by relatively brief excursions of rapid magnetic field variation. With respect to time duration, the local enhancements generally occurred over a period of 2-5 minutes. (See **Figures I-8 – I-11**)

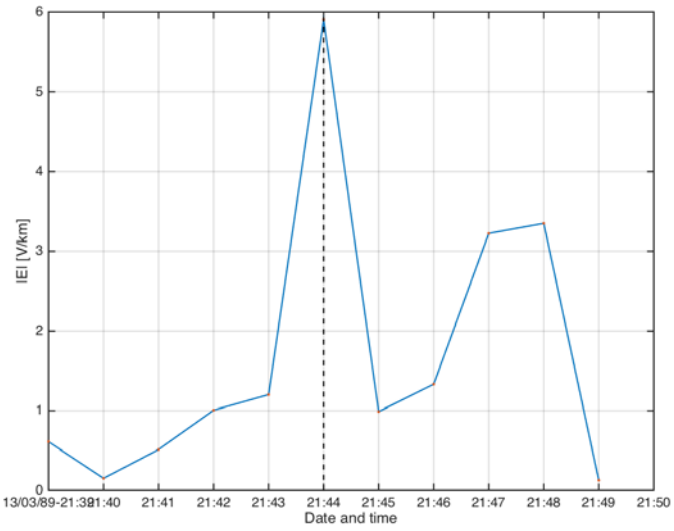

Figure I-8: Geoelectric field March 13, 1989, at 21:44 UT, Brorfelde (BFE), Denmark.

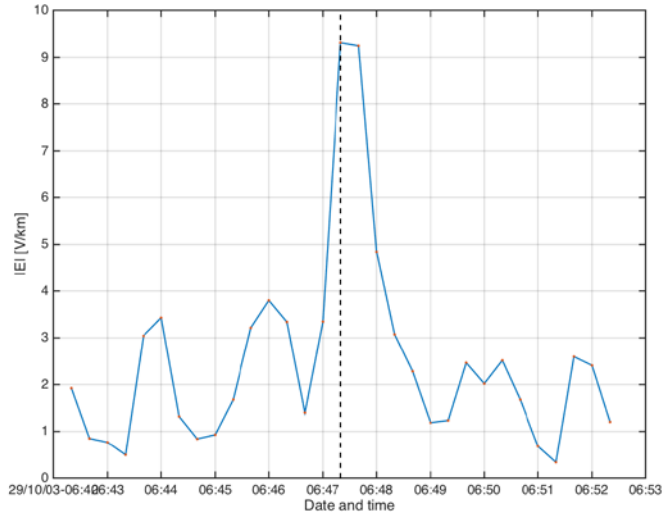

Figure I-9: Geoelectric field October 29, 2003, at 06:47 UT, Narsarsuaq (NAQ), Greenland

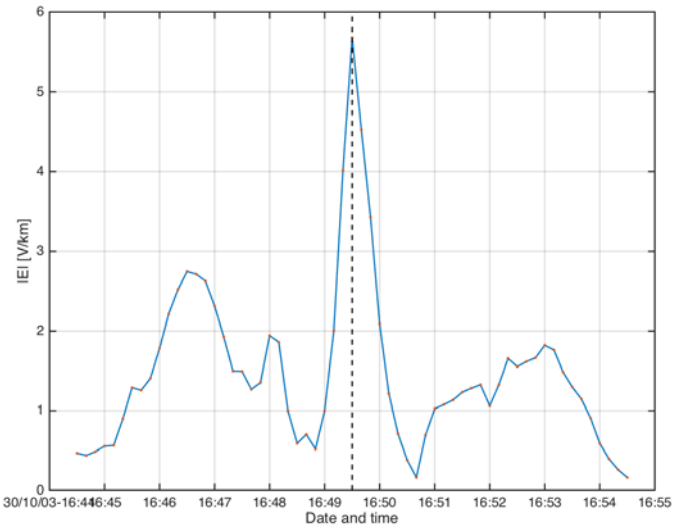

Figure I-10: Geoelectric field October 30, 2003, at 16:49UT, Hopen Island (HOP), Norway

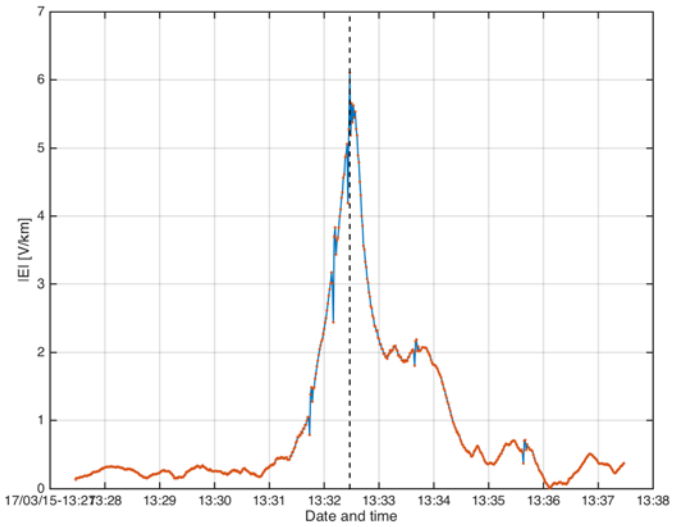

Figure I-11 – Geoelectric field March 17, 2015, at 13:33 UT, Deadhorse, Alaska

Based on the above analysis and the previous work associated with the benchmark GMD event, it is reasonable to incorporate a second (or supplemental) assessment into TPL-007 to account for the potential impact of a local enhancement in both the network analysis and the transformer thermal assessment(s).

With respect to geographic area of the localized enhancement, the historical geomagnetic field data analyzed so far provides some insight. Analysis suggests that the enhancements will occur in a relatively narrow band of geomagnetic latitude (on the order of 100 km) and wider longitudinal width (on the order of 500 km) as a consequence of the westward-oriented structure of the source in the ionosphere.

Proposed TPL-007-2 provides flexibility for planners to determine how to apply the supplemental GMD event to the planning area. Acceptable approaches include but are not limited to:

- Apply the peak geoelectric field for the supplemental GMD event (12 V/km scaled to the planning area) over the entire planning area;

- Apply a spatially limited (e.g., 100 km in North-South direction and 500 km in East-West direction) geoelectric field enhancement (12 V/km scaled to the planning area) over a portion(s) of the system, and apply the benchmark GMD event over the rest of the system.
- Other methods to adjust the benchmark GMD event analysis for localized geoelectric field enhancement.

Given the current state of knowledge regarding the spatial extent of a local geomagnetic field enhancements, upper geographic boundaries, such as the values used in the approaches above, are reasonable but are not definitive.

Local Enhancement Waveform

The supplemental geomagnetic field waveform was derived by modifying the benchmark GMD event waveform to emulate the observed events described above. The temporal location of the enhancement corresponds to the time of the benchmark event with the highest geoelectric field. The local enhancement was constructed by scaling linearly a 5-minute portion of the benchmark geomagnetic field so that the peak geoelectric field is 12 V/km at a geomagnetic latitude of 60° and reference earth model. **Figure I-12** shows the benchmark geomagnetic field and **Figure I-13** shows the supplemental event geomagnetic field. **Figure I-14** expands the view into B_x, with and without the local enhancement. **Figure I-15** is the corresponding expanded view of the geoelectric field magnitude with and without the local enhancement.

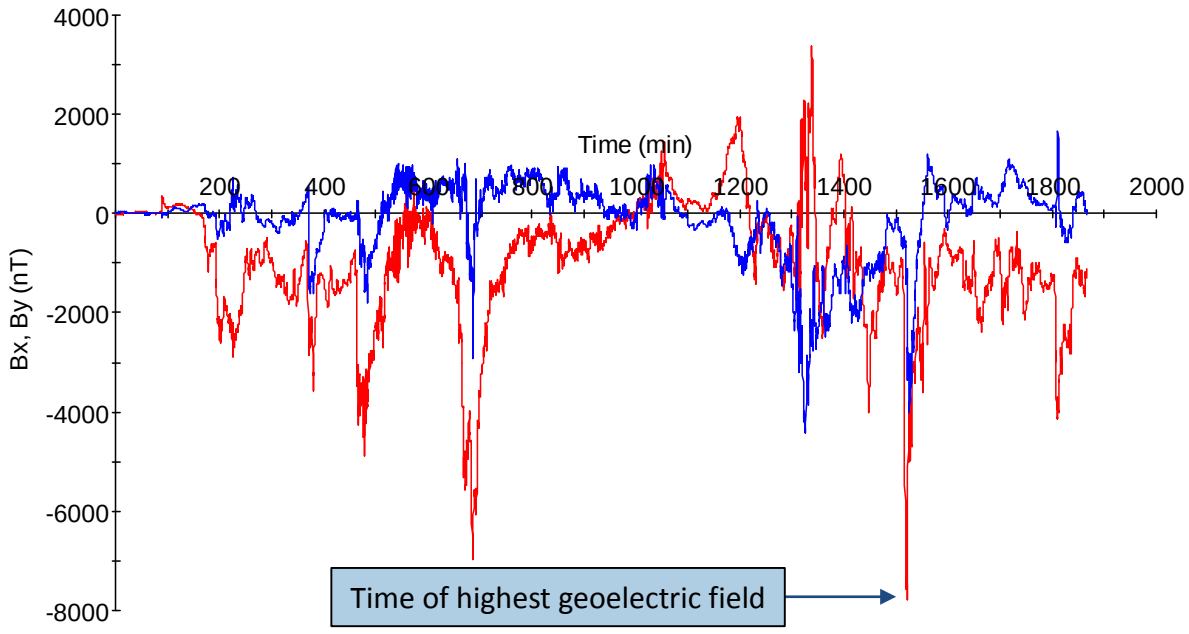

Figure I-12: Benchmark Geomagnetic Field. Red B_x (Northward), Blue B_y (Eastward)

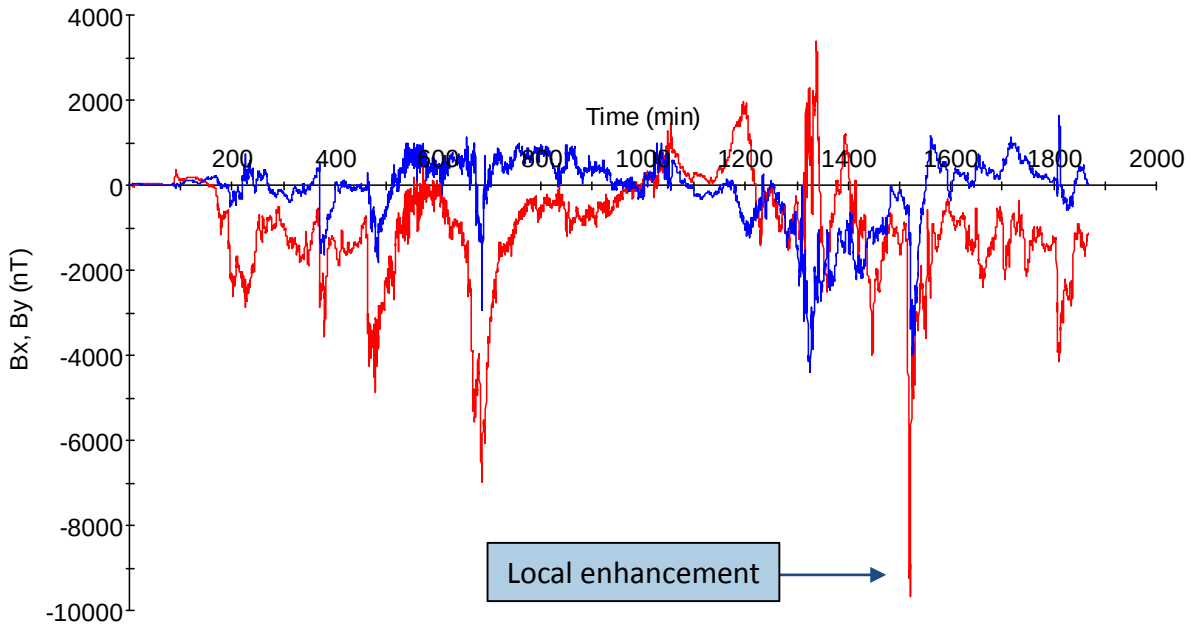

Figure I-13: Supplemental Geomagnetic Field Waveform. Red B_x (Northward), Blue B_y (Eastward)

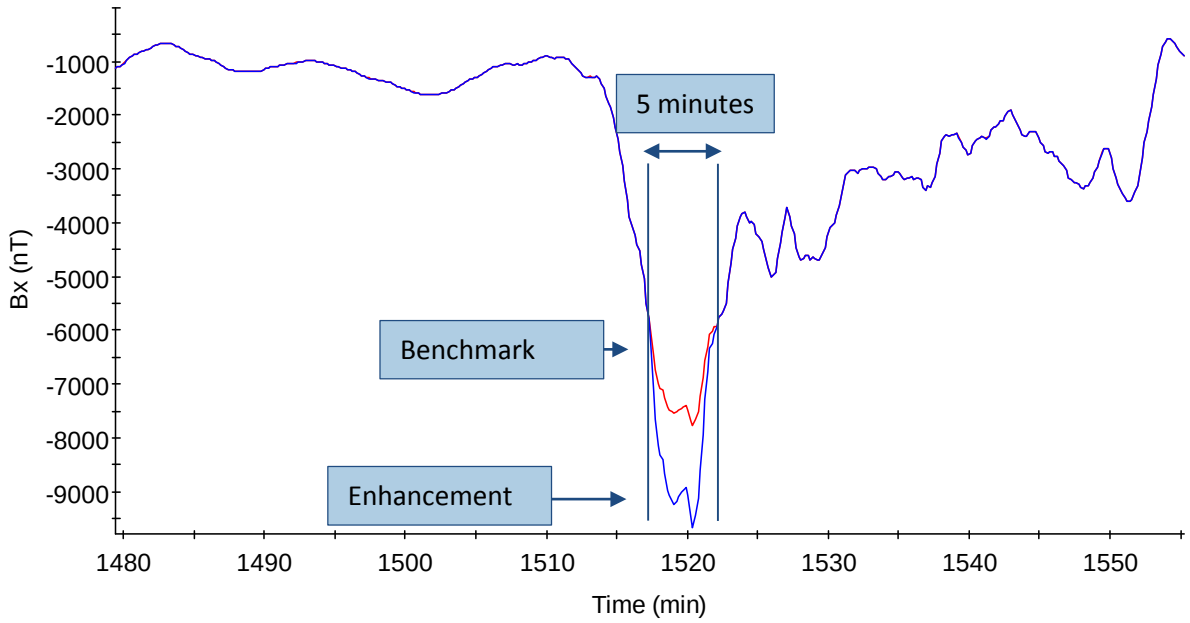

Figure I-14: Red Benchmark B_x and Blue Supplemental B_x (Northward) – Expanded View

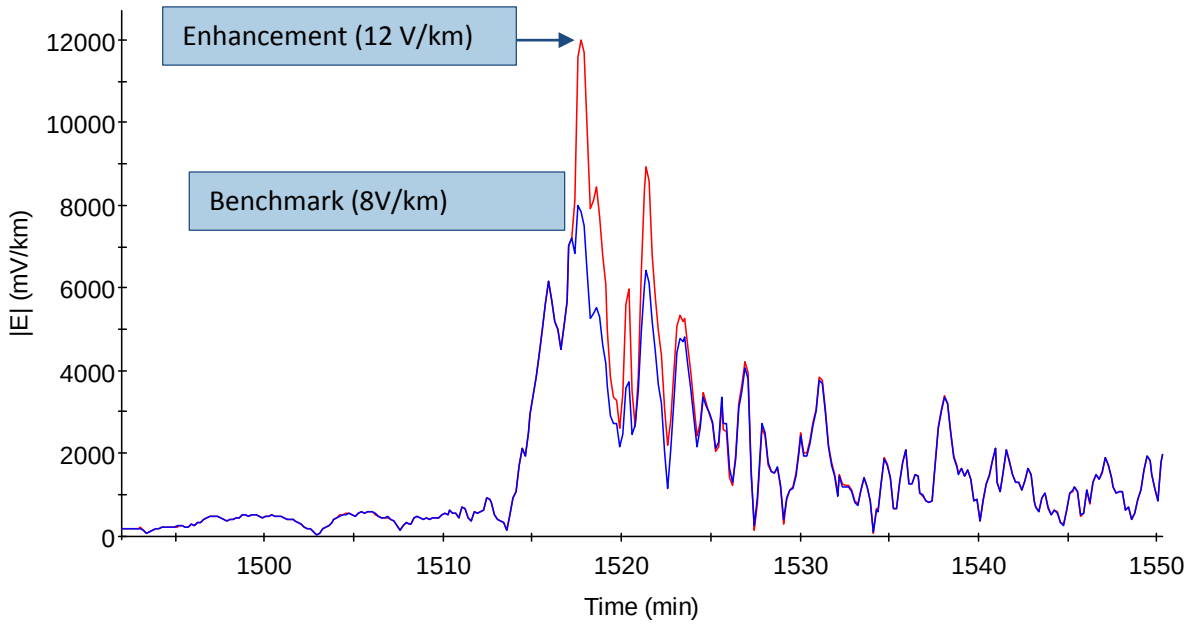

Figure I-15: Magnitude of the Geoelectric Field. Benchmark Blue and Supplemental Red – Expanded View

Transformer Thermal Assessment

The local enhancement of the supplemental GMD event waveform can have a material impact on the temperature rise (hot-spot heating or metallic parts) even though the duration of the local enhancement is approximately 5 minutes. Thermal assessments based on the supplemental GMD event can be performed using the same methods employed for benchmark thermal assessments.[9]

[9] See Transformer Thermal Impact Assessment white paper: http://www.nerc.com/pa/Stand/Pages/Project-2013-03-Geomagnetic-Disturbance-Mitigation.aspx

Appendix II – Scaling the Supplemental GMD Event

The intensity of a GMD event depends on geographical considerations such as geomagnetic latitude and local earth conductivity [2].[10] Scaling factors for geomagnetic latitude take into consideration that the intensity of a GMD event varies according to latitude-based geographical location. Scaling factors for earth conductivity take into account that the induced geoelectric field depends on earth conductivity, and that different parts of the continent have different earth conductivity and deep earth structure.

Scaling the supplemental GMD event differs from the benchmark GMD event in two ways:

- E_{peak} is 12 V/km instead of 8 V/km
- Beta factors for scaling the geoelectric field based on earth conductivity are different (see **Table II-2**)

More discussion, including example calculations, is contained in the Benchmark GMD Event Description white paper.

Scaling the Geomagnetic Field

The supplemental GMD event is defined for geomagnetic latitude of 60° and it must be scaled to account for regional differences based on geomagnetic latitude. To allow usage of the supplemental geomagnetic field waveform in other locations, **Table II-1** summarizes the scaling factor α correlating peak geoelectric field to geomagnetic latitude as described in **Figure II-1** [3]. This scaling factor α has been obtained from a large number of global geomagnetic field observations of all major geomagnetic storms since the late 1980s [15]-[27], and can be approximated with the empirical expression in (II.1)

$$\alpha = 0.001 \cdot e^{(0.115 \cdot L)} \qquad \text{(II.1)}$$

where L is the geomagnetic latitude in degrees and $0.1 \leq \alpha \leq 1.0$.

[10] Geomagnetic latitude is analogous to geographic latitude, except that bearing is in relation to the magnetic poles, as opposed to the geographic poles. Geomagnetic phenomena are often best organized as a function of geomagnetic coordinates. Local earth conductivity refers to the electrical characteristics to depths of hundreds of km down to the earth's mantle. In general terms, lower ground conductivity results in higher geoelectric field amplitudes.

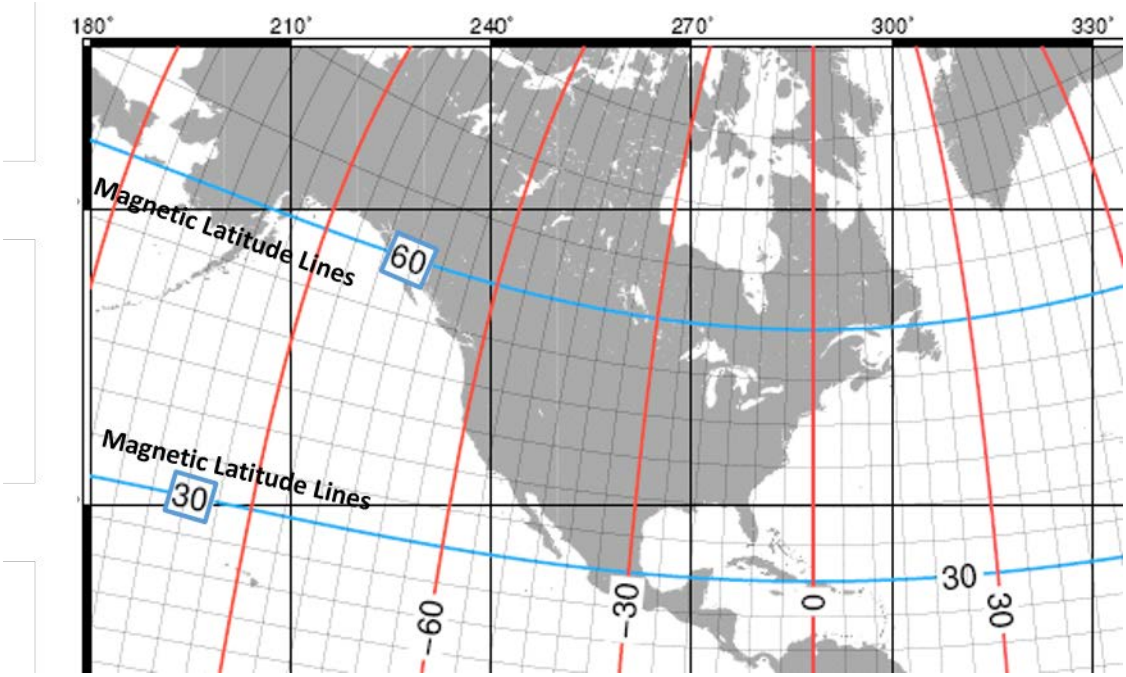

Figure II-1: Geomagnetic Latitude Lines in North America

Table II-1: Geomagnetic Field Scaling Factors

Geomagnetic Latitude (Degrees)	Scaling Factor1 (α)
≤ 40	0.10
45	0.2
50	0.3
54	0.5
56	0.6
57	0.7
58	0.8
59	0.9
≥ 60	1.0

Scaling the Geoelectric Field

The supplemental GMD event is defined for the reference Quebec earth model provided in **Table 1**. This earth model has been used in many peer-reviewed technical articles [11, 15]. The peak geoelectric field depends on the geomagnetic field waveform and the local earth conductivity. Ideally, the peak geoelectric field, E_{peak}, is obtained by calculating the geoelectric field from the scaled geomagnetic field waveform using the plane wave method and taking the maximum value of the resulting waveforms

$$E_N = (z(t)/\mu_o) * B_E(t)$$
$$E_E = -(z(t)/\mu_o) * B_N(t) \quad \text{(II.2)}$$
$$E_{peak} = \max\left\{\left|E_E(t), E_N(t)\right|\right\}$$

where,

* denotes convolution in the time domain,

z(t) is the impulse response for the earth surface impedance calculated from the laterally uniform or 1D earth model,

$B_E(t)$, $B_N(t)$ are the scaled Eastward and Northward geomagnetic field waveforms,

$E_E(t)$, $E_N(t)|$ are the magnitudes of the calculated Eastward and Northward geoelectric field $E_E(t)$ and $E_N(t)$.

As noted previously, the response of the earth to B(t) (and dB/dt) is frequency dependent. **Figure II-2** shows the magnitude of Z(ω) for the reference earth model.

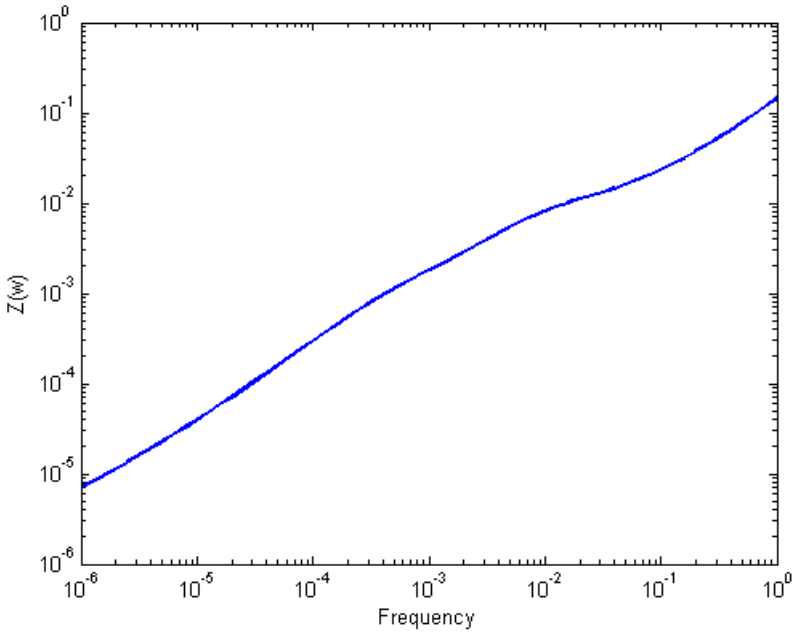

Figure II-2: Magnitude of the Earth Surface Impedance for the Reference Earth Model

If a utility does not have the capability of calculating the waveform or time series for the geoelectric field, an earth conductivity scaling factor β_S can be obtained from **Table II-2**. Using α and β, the peak geoelectric field E_{peak} for a specific service territory shown in **Figure II-3** can be obtained using (II.3)

$$E_{peak}\ 12 \times \alpha \times \beta_s \text{ (V/km)} \quad \text{(II.3)}$$

It should be noted that (II.3) is an approximation based on the following assumptions:

- The earth models used to calculate Table II-2 for the United States are from published information available on the USGS website. These scaling factors are slightly lower than the ones in the benchmark because the supplemental benchmark waveform has a higher frequency content at the time of the local enhancement.
- The models used to calculate Table II-2 for Canada were obtained from NRCan and reflect the average structure for large regions. When models are developed for sub-regions, there will be variance (to a greater or lesser degree) from the average model. For instance, detailed models for Ontario have been developed by NRCan and consist of seven major sub-regions.
- The conductivity scaling factor β_S is calculated as the quotient of the local geoelectric field peak amplitude in a physiographic region with respect to the reference peak amplitude value of 12 V/km. Both geoelectric field peak amplitudes are calculated using the supplemental geomagnetic field time series. If a different geomagnetic field time series were used, the calculated scaling factors (β) would be different than the values in Table II-2 because the frequency content of storm maxima is, in principle, different for every storm. If a utility has technically-sound earth models for its service territory and sub-regions thereof, then the use of such earth models is preferable to estimate E_{peak}.
- When a ground conductivity model is not available the planning entity should use the largest β_s factor of adjacent physiographic regions or a technically-justified value.

Physiographic Regions of the Continental United States

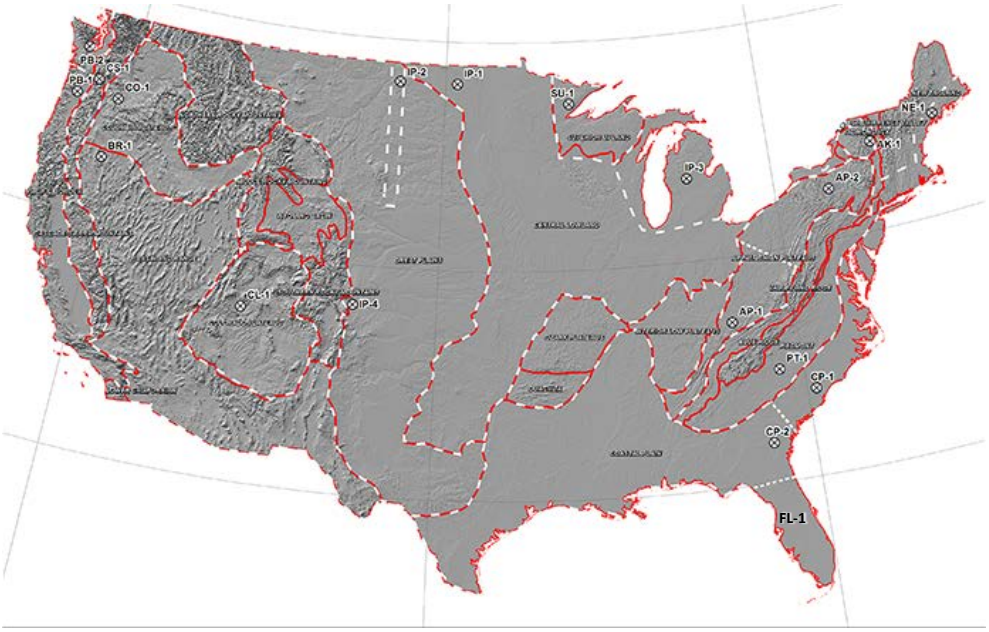

Physiographic Regions of Canada

Figure II-3: Physiographic Regions of North America

Table II-2 Supplemental Geoelectric Field Scaling Factors	
Earth model	**Scaling Factor (β)**
AK1A	0.51
AK1B	0.51
AP1	0.30
AP2	0.78
BR1	0.22
CL1	0.73
CO1	0.25
CP1	0.77
CP2	0.86
FL1	0.73
CS1	0.37
IP1	0.90
IP2	0.25
IP3	0.90
IP4	0.35
NE1	0.77
PB1	0.55
PB2	0.39
PT1	1.19
SL1	0.49
SU1	0.90
BOU	0.24
FBK	0.56
PRU	0.22
BC	0.62
PRAIRIES	0.88
SHIELD	1.0
ATLANTIC	0.76

References

[1] *High-Impact, Low-Frequency Event Risk to the North American Bulk Power System*, A Jointly-Commissioned Summary Report of the North American Reliability Corporation and the U.S. Department of Energy's November 2009 Workshop.

[2] Application Guide: Computing Geomagnetically-Induced Current in the Bulk-Power System, NERC. NERC. http://www.nerc.com/comm/PC/Geomagnetic%20Disturbance%20Task%20Force%20GMDTF%202013/GIC%20Application%20Guide%202013_approved.pdf

[3] Kuan Zheng, Risto Pirjola, David Boteler, Lian-guang Liu, "Geoelectric Fields Due to Small-Scale and Large-Scale Source Currents", *IEEE Transactions on Power Delivery*, Vol. 28, No. 1, January 2013, pp. 442-449.

[4] Boteler, D. H. "Geomagnetically Induced Currents: Present Knowledge and Future Research", *IEEE Transactions on Power Delivery*, Vol. 9, No. 1, January 1994, pp. 50-58.

[5] Boteler, D. H. "Modeling Geomagnetically Induced Currents Produced by Realistic and Uniform Electric Fields", *IEEE Transactions on Power Delivery*, Vol. 13, No. 4, January 1998, pp. 1303-1308.

[6] J. L. Gilbert, W. A. Radasky, E. B. Savage, "A Technique for Calculating the Currents Induced by Geomagnetic Storms on Large High Voltage Power Grids", Electromagnetic Compatibility (EMC), 2012 IEEE International Symposium on.

[7] *How to Calculate Electric Fields to Determine Geomagnetically-Induced Currents.* EPRI, Palo Alto, CA: 2013. 3002002149.

[8] Pulkkinen, A., R. Pirjola, and A. Viljanen, Statistics of extreme geomagnetically induced current events, *Space Weather*, 6, S07001, doi:10.1029/2008SW000388, 2008.

[9] Boteler, D. H., Assessment of geomagnetic hazard to power systems in Canada, *Nat. Hazards*, 23, 101–120, 2001.

[10] Finnish Meteorological Institute's IMAGE magnetometer chain data available at: http://image.gsfc.nasa.gov/

[11] Boteler, D. H., and R. J. Pirjola, The complex-image method for calculating the magnetic and electric fields produced at the surface of the Earth by the auroral electrojet, *Geophys. J. Int.*, 132(1), 31—40, 1998

[12] Coles, Stuart (2001). An Introduction to Statistical Modelling of Extreme Values. Springer.

[13] Pulkkinen, A., A. Thomson, E. Clarke, and A. Mckay, April 2000 geomagnetic storm: ionospheric drivers of large geomagnetically induced currents, *Annales Geophysicae*, 21, 709-717, 2003.

[14] Pulkkinen, A., S. Lindahl, A. Viljanen, and R. Pirjola, Geomagnetic storm of 29–31 October 2003: Geomagnetically induced currents and their relation to problems in the Swedish high-voltage power transmission system, *Space Weather*, 3, S08C03, doi:10.1029/2004SW000123, 2005.

[15] Pulkkinen, A., E. Bernabeu, J. Eichner, C. Beggan and A. Thomson, Generation of 100-year geomagnetically induced current scenarios, *Space Weather*, Vol. 10, S04003, doi:10.1029/2011SW000750, 2012.

[16] Ngwira, C., A. Pulkkinen, F. Wilder, and G. Crowley, Extended study of extreme geoelectric field event scenarios for geomagnetically induced current applications, *Space Weather*, Vol. 11, 121–131, doi:10.1002/swe.20021, 2013.

[17] Thomson, A., S. Reay, and E. Dawson. Quantifying extreme behavior in geomagnetic activity, *Space Weather*, 9, S10001, doi:10.1029/2011SW000696, 2011.